High magnetic field effect in organic light emitting diodes

Yuichiro Goto[1], Takuya Noguchi[1], Utahito Takeuchi[1], Kunitada Hatabayashi[1], Yasushi Hirose[1], Takayuki Uchida[2], Takehiko Sasaki[3], Tetsuya Hasegawa[1], Toshihiro Shimada[4*]

[1] Department of Chemistry, The University of Tokyo, Bunkyo-ku, Tokyo 113-0033, Japan

Tokyo

[2] Department of Media and Image Technology, Tokyo Polytechnic University, Atsugi, 243-0297, Japan

[3] Department of Complexity Science and Engineering, The University of Tokyo, Kashiwa 277-8561, Japan

[4] Department of Materials Chemistry, Faculty of Engineering, Hokkaido University, Sapporo 060-8628, Japan

Abstract

Fluorescent and phosphorescent organic light emitting diodes (OLEDs) were measured in high magnetic field up to 9 T. The current efficiency steeply increased below 100mT as reported but gradually decreased when the field was larger. In the range of 0.1 - 6.5 T, the decrease was proportional to the square of the magnetic field, whereas in the range between 6.5T and 9T, it was proportional to the square root of the magnetic field. In contrast, phosphorescent OLED did not show magnetic field dependence. Unipolar devices of n-type Alq_3 (Tris-(8-hydroxyquinolino) aluminum) and p-type α-NPD (N',N'-Di(naphthalene-1-yl)-N,N' dipheyl-benzidine) showed positive linear magnetoresistance only for minority carriers. The mechanism of the quadratic dependence of the electroluminescent intensity is discussed based on the experimental results.

Introduction

Magnetic field effect (MFE) on organic light emitting diodes (OLEDs) have been attracting research activities for the development of more efficient OLEDs and for understanding the behavior of spins in organic semiconductors. The reports on MFE of OLEDs without ferromagnetic component qualitatively agree with each other, *i.e.*, steep increase (2~10%) in the low magnetic field (< 100mT) and gradual decrease in the higher magnetic field. Although the behavior in the low magnetic field region is intensively studied and complicated phenomena including magnetoresistance are being elucidated [1-14], very few experiments in relation to the MFE on organic semiconductors have been performed under high magnetic field larger than 2T [15].

The reported mechanisms in the MFE are analyzed based on the chemistry of radical pairs: hyperfine coupling (hfc), difference in *g*-factors (Δg), triplet-triplet annihilation (TTA) are typically mentioned in the literature, all of which are relavant to the dynamics of a singlet(S) or a triplet(T) radical pair (a neighboring pair of cation and anion) converting to S and T excitons, with mixing of the spin states. The detailed description of them will be found in the literature [1-16]. It should be noted here that all of the above mentioned mechanisms exhibit *concave* curves of the emission efficiency as a function of external magnetic field (B). The MFEs on electroluminescent efficiency by those mechanisms are schematically drawn in Fig. 1 [16].

Since some of the exciton-related effects saturate at relatively low magnetic field (~ 1T), it is expected that the contribution of the above mechanisms in MFE will be separated if high magnetic field is applied. In this paper, we measured MFE of fluorescent and phosphorescent OLEDs up to 9T and discuss the origin of observed MFE in the high magnetic field. It seems that the results cannot be explained by the known exciton-related mechanisms (Δg, hfc, TTA etc.), and the origin is discussed based on the transport characteristics.

Experiments

Sample preparation

The structure of fluorescent device is shown in Fig. 2(a). An indium tin oxide (ITO) coated glass substrate (purchased from Aldrich) with a sheet resistivity of 8-12 Ω/square was used as the substrate. 100nm N',N'-Di(naphthalene-1-yl)-N,N' dipheyl-benzidine (α-NPD) and 100nm Tris-(8-hydroxyquinolino) aluminum (Alq_3) were deposited successively as the hole transporting layer and emitting / electron transporting layer, respectively. Then a cathode was deposited consisting of a 2 nm Cs layer followed by 150 nm of Al. The ITO substrate was cleaned by ultrasonicating in ethanol and acetone. Following this, the ITO was treated in ozone for 20 min. The α-NPD and Alq_3 were purchased from Luminescence Technology Corporation. The deposition of the organic layers was performed using Knudsen-cells in a vacuum chamber with a base pressure during evaporation of ~10^{-7} Torr. . Cs was deposited with alkali metal dispenser (purchased from SAES Getters). The deposition rate of organic materials was about 0.1 nm/s. Calibrated quartz crystal microbalances were used to determine the deposition rate. The structure of phosphorescence device is shown in Fig. 2(b). Doping of 5% $Btp_2Ir(acac)$ in CBP was performed by controlling the evaporation rate by monitoring the quartz crystal microbalances.

The sample OLEDs and unipolar devices were transferred from the deposition chamber to glove box filled with dry N_2 (concentration of H_2O and oxygen was less than 100 ppm) without exposing them to air. The electrical connection to the OLED was made using 20 μm-diameter Cu wire with In contact. Then the OLED sample was sealed in a glass box using photo-hardening epoxy (Threebond 3124) together with a zeolite desiccant (Shinagawa Kasei Co. LTD).

Measurement

MFE was measured at 300K in superconducting magnet using Physical Property Measurement

System (PPMS; Quantum Design). The magnetic field was perpendicular to the device plane. The magnetic field was increased from 0 T to 9 T and then was decreased from 9 T to 0 T in order to check the temporal changes. The results are shown after confirming pure MFE is observed, unless stated otherwise. The emission intensity was measured with photon counter H7155-21 (Hamamatsu Photonics) in magnetic shielding made of thick iron plates and cylinders. The shielding of photon counter was tested by introducing light with various intensities by optical fiber to make sure there was no magnetic field dependence on its output. The bias was applied by the Keithley 6487 picoammeter / voltage source in constant voltage mode.

Results

Fluorescent OLED

First we show the characteristics of the fluorescent device without applying the magnetic field. Figure 3 shows the emission intensity and current of the fluorescent and phosphorescent OLED as a function of voltage. It is reported that TTA in Alq_3-based fluorescent OLEDs occurs when the current density is larger than 100 mA/cm^2 [17] and some of our measurement exceeds this limit. However, since the magnetic field dependence of TTA appears only at low temperatures [13-14], we consider we can neglect contribution from TTA in the present measurement at 300 K.

The emission intensity, current and emission efficiency of the same device under the magnetic field are shown in Fig. 4. The emission intensity and current show different magnetic field dependence on the sweep direction (0 -> 9T / 9 -> 0T) (Fig 4 (a)(b)). However, their ratio, i.e. emission efficiency, does not show the hysteresis as shown in Fig. 4(c). It means that the hysteresis comes from the charge injection process from the electrodes to the emission layer. We found that the "hysteresis" is dependent on both of the magnetic field and the time from the start of the current flow. The time dependence is probably due to the bias stress on the device, but the magnetic field

dependence might be related with MFE of the trap / detrap processes.

The emission efficiency (and also the emission intensity and the current) increase steeply as a function of *B* when it was less than 0.02 T as reported in the literature, and gradually decreases as *B* was further increased. It should be noted that the decrease in the mid~ high *B* region is *convex* function, which cannot be explained by widely accepted behavior of hfc, Δg and TTA mechanisms which exhibit *concave* behavior against *B*. We will discuss this point later.

In order to see dependence on *B* more clearly, we re-plotted Fig. 4(c) as a function of B^2. Figure 5(a) clearly shows the linear decrease of the fluorescent efficiency against B^2 in the range of 0.1 T~ 6.5 T. On the other hand, by re-plotting Fig 4(c) as a function of $B^{1/2}$ (Fig. 5(b)), it is noticed that the decrease of the emission efficiency shows $B^{1/2}$ dependence in the range of 6.5 T ~ 9 T.

Phosphorescent OLED

Figure 6 shows the MFE on the emission efficiency of the phosphorescent OLED. In contrast to the results of the fluorescent device, it did not show the magnetic field dependence. Although we changed the driving voltage (4V, 6V, 8V, 10V), the magnetic field dependence did not appear.

Magnetoresistance measurement of unipolar devices

In order to investigate the charge balance factor which might influence the EL efficiency, we measured the magnetoresistance of the majority and minority carriers in α-NPD and Alq_3 by making the unijunction devices with different work function electrodes (Au and Cs). All of the devices showed Ohmic *I* -*V* characteristics in the measured range (-10~10V). The results of MFE on the current at constant voltage are shown in Figs. 6(a)-(d). The voltages were chosen to give current in the range of 10~100 μA and the results are shown after normalization at zero field. It is easily noticed that the MFEs on the conductivity of the majority carriers (holes in α-NPD and electrons in

Alq_3) are negligible, whereas linear decreases in the conductivity was observed for the minority carriers (electrons in α-NPD and holes in Alq_3). Since the *I-V* characteristics are Ohmic, it shows the mobility values of the minority carriers decrease linearly as a function of the magnetic field.

Discussions

We found the decrease in the fluorescent efficiency in organic EL devices proportional to B^2 in the range of 0.1~6.5T. Such dependence has not been reported to the authors' knowledge.

The EL efficiency (η_{ext}) is given by the following:

$$\eta_{ext} = \alpha \times \Phi_{PL} \times \Phi_{exciton} \times \gamma \qquad (1)$$

Here, α, Φ_{PL}, $\Phi_{exciton}$, γ are the light extra efficiency, quantum efficiency of organic material, exciton formation efficiency, and carrier balance factor, respectively.

α is related with the magnetic field via Faraday /Kerr effects with interference. The Faraday rotation of the non-magnetic and thin organic layers is not significant even at 9T and interference would not change as a function of magnetic field. Thus we can neglect α. The fluorescent in optically excited organic dyes in the magnetic field has been studied in detail [18], but B^2 dependence in high magnetic field was not reported in the literature. Therefore, our result cannot be explained by Φ_{PL}. Since all known mechanism of MFE on $\Phi_{exciton}$ gives concave dependence on B as mentioned earlier, we here tentatively rule out the contribution from $\Phi_{exciton}$ as the main mechanism of the present B^2 dependence.

The remaining factor in eq. (1) is the charge balance factor. We examined various models to relate the MFE on the charge balance factor, and the following is the only model that can barely explain the B^2 dependence. We observed that the conductance of the minority carrier changes linearly as a function of magnetic field as shown in Fig. 6. We considered various models based on our observation (Fig. 7) that the mobility of the minority carrier (μ) depends upon the magnetic field

(B) as

$$\mu = \mu_0 (1 - aB) \qquad (2)$$

where μ_0 and a are materials dependent constants. Since the EL intensity is determined only by the charge balance if the carrier recombination rate is proportional to the radiation [19], eq. (2) gives the fluorescent efficiency linearly related with B^1. However, our experiments showed that the current remains almost constant as a function of the magnetic field in the mid ~ high B range. We have found that we can deduce the B^2 dependence from eq. (2) with additional two assumptions. The assumptions are as follows. (i) The emission region is very narrow and only the recombination at this region contributes to the emission. This is reasonable because Alq_3 layer (200nm) is much thicker than the thickness of emission region of ordinary devices [20]. The interfacial mixing and the damage caused by the electrode formation might also justify this assumption. (ii) The hole current (J_h) and electron current (J_e) are balanced in the emission region when $B = 0$. Since the mobility of the majority carrier is smaller in Alq_3 than α-NPD [21,22], it is believed that the recombination and the emission occurs in Alq_3. This assumption is also reasonable because the device characteristics (Fig. 3), in which turn-on voltage of current is almost the same as that of emission intensity, show that this device has good carrier balance.

Since the current is constant as a function of B, $J_h + J_e$ is constant. From the assumption (ii), $J_h = J_e$ at the emission region when B=0. The emission region is in Alq_3 and Eq.(2) becomes

$$J_h = J_0(1-aB),$$

where J_0 is a constant.

Because J_h+J_e is constant, J_e at the emission region can be written as

$$J_e=J_0(1+aB).$$

The recombination rate is proportional to J_hJ_e

$$J_hJ_e = J_0^2 (1-aB)(1+aB) = J_0^2 (1-a^2B^2)$$

and the decrease of the emission proportional to B^2 is explained.

Although this model is based on several assumptions which are not commonly considered so far, we could not think of better ones. We understand that the carrier transport of unipolar devices are not the same as the bipolar devices, for example, charge injection at the electrodes might be strongly involved in the minority carriers. However, our finding of linear MFE on minority carriers has not been reported and no theoretical prediction has been made to the author's knowledge. There might exist other mechanisms which also explain these results, but we hope the present result and discussions may stimulate the study of MFE on organic semiconductors and devices. Although TTA is not likely to work at room temperature and hfc will saturate at relatively low magnetic field, ΔG works at high magnetic field region and might be cooperative with other factors.

There is another mechanism which might explain the B^2 dependence, although it is not consistent with the results on the unipolar devices (eq.(2)). It is theoretically predicted that the decrease of the conductivity proportional to B^2 is characteristics of magnetoresistance of hopping transport and that it levels off to the B^1 dependence when the magnetic field is high [21]. If it is applicable to the carriers in the emission layer of an OLED, the charge balance of the device will change in the same manner as the conductance and the emission decrease proportional to B^2 will be observed. The difficulty of this model is that we did not see such magnetoconductance in unipolar devices with *n*-type, and *p*-type organic single layers.

In the range beyond 6.5T, we observed $B^{1/2}$ dependence (Fig. 5(b)). In the study of the radical pair in solution, it is known that the density of singlet excitons decreases in proportion to $B^{1/2}$ by Δg mechanism [23]. The magnetoconductance of the minority carriers shown in Fig. 7 start to saturate in the range beyond 6.5 T. Although we do not know the mechanism of this saturation, it might be the reason why $B^{1/2}$ dependence due to Δg mechanism start to appear in this region.

Conclusion

We measured EL efficiency of fluorescent and phosphorescent OLEDs in the magnetic field up to 9T and we found quadratic decrease as a function of the magnetic field between 0.1 ~ 6.5T. We also measured magnetoconductance of unipolar devices and observed that only minority carriers show significant magnetoconductance decreasing linearly with the magnetic field (15% at 9T in Alq_3). $B^{1/2}$ dependence in the range beyond 6.5T can be explained by MFE on the density of singlet exciton caused by Δg mechanism.

Acknowledgment

This work was supported by GCOE "Chemistry Innovation through Collaboration of Science and Technology" from MEXT, Japan and Shorai Science and Technology Foundation.

References

[1]J.Kalinowski, in Organic Electroluminescent Materials and Devices, Gordon Publishers, New York, 1997.

[2] J.Kalinowski, M.Cocchi, D.Virgili, P.D.Marco, V.Fattori, Chem. Phys. Lett. 380 (2003) 710.

[3] J.Kalinowski, M.Cocchi, D.Virgili, V.Fattori, P.D.Marco, Phys. Rev. B 70 (2004) 205303.

[4] Y.Sakaguchi, Y.Iwasaki, T.Osasa, M.Asahi, M.Matsumura, Phys. Rev. B 74 (2006) 195209.

[5]A.H.Davis, K.Bussmann, J. Vac. Sci. Technol. A 22 (2004) 1885.

[6]H.Okada, Y.Okimoto, T.Yamada, H.Okamoto, M.Kawasaki, Y.Tokura, Appl. Phys. Lett, 88 (2006) 123501.

[7] B.Hu, Y.Wu, Nature Mat. 6 (2007) 985.

[8]P.Desai, P.Shakya, T.Kreouzi, W.P.Gillin, J. Appl. Phys. 102 (2007) 073710.

[9] Y.Shemg, T.D.Nguyen, G.Veeraraghavan, O.Mermer, Phys. Rev. B 75 (2007) 035202.

[10]P.Shakya, P.Desai, M.Somerton, G.Gannaway, T.Kreouzis, W.P.Gillin, J. Appl. Phys. 103 (2008) 103175.

[11]P.A.Bobbert, T.D.Nguyen, F.W.A.van Oost, B.Koopmans, M.Wohlgenannt, Phys. Rev. Lett. 99 (2007) 216801.

[12] P.Desai, P.Shakya, T.Kreouzis, W.P.Gillin, Phys. Rev. B 75 (2007) 094423.

[13]Y.L.Lei, Y.Zhang, R.Lui, P.Chen, Q.L.Song, Z.H.Xiong, Organic Electronics 10 (2009) 889.

[14]R.Liu, Y.Zhang, Y.L.Lei, P.Chen, Z.H.Xiong, J. Appl. Phys. 105 (2009) 093719.

[15] M.Reufer, M.J.Walter, P.G.Lagoudakis, A.B.Hummel, H.S.Kolb, H.G.Roskos, U.Scherf, J.M.Lupton, Nature Mat. 4 (2005) 340.

[16] H.Hayashi, Y.Sakaguchi, J. Photochem. Photobiol. C : Photochem. Reviews,6 (2005) 25.

[17] D.Y. Kondakov, J. Appl. Phys. 102 (2007) 114504.

[18] R. Katoh, M. Kotani, Chem. Phys. Lett. 196 (1992) 108.

[19] J.C. Scott, S. Karg, S.A. Carter, J. Appl. Phys. 82 (1997) 1454.

[20] C.W. Tang, S.A. Vanslyke, C.H. Chen, J. Appl. Phys 65 (1989) 3610.

[21] R. G. Kepler, P. M. Beeson, S. J. Jacobs, R. A. Anderson, M. B. Sinclair, V. S. Valencia, P. A. Cahill, Appl. Phys. Lett, 66 (1995) 3618.

[22] N. D. Nguyen, M. Schmeits, H. P. Loebl, Phys. Rev. B 75 (2007) 075307.

[23]Y.Sakaguchi, H.Hayashi, Chem. Phys. Lett. 245 (1995) 591.

Figure Captions

Fig.1: Schematic drawing of the magnetic field effect on singlet exciton yield. (a)hyperfine coupling (hfc) (b)difference in the g-factor (Δg) (c)triplet-triplet annihilation (TTA)

Fig.2 Device structures (a)fluorescent device (b)Phosphorescent device. The abbreviations are as follows. BCP: 2,9-dimethyl-4,7-diphenyl-phenanthroline, Btp2Ir(acac): bis(2-(2'-benzo[4,5-α]thienyl) pyridinato-N,C^{3}') iridium (acetyl-acetonate), CBP: 4,4'-N,N'-dicarbazole-diphenyl

Fig.3: Normalized emission intensity and current density as a function of the voltage without applying the magnetic field (0T) (a) fluorescent device (b) phosphorescent device

Fig.4: Magnetic field effect of the fluorescent device (normalized at zero field). ((a) Emission Intensity, (b) Current, (c) Emission Efficiency at 4V). The arrows show the sweep direction of the magnetic field (0-9T / 9-0T).

Fig.5: Normalized emission efficiency of the fluorescent device plotted against (a) B^2 (b) $B^{1/2}$.

Fig.6 Magnetic field effect of the phosphorescent device (normalized at zero field). The result at 10V is shown in the inset.

Fig.7 Magnetic field effect of conductance of unipolar devices (normalized at zero field). (a)Au/α-NPD/Au (holes) (b)Au/Cs/α-NPD/Cs/Au (electrons) (c)Au/Cs/Alq_3/Cs/Au (electrons) (d)Au/Alq_3/Au (holes)

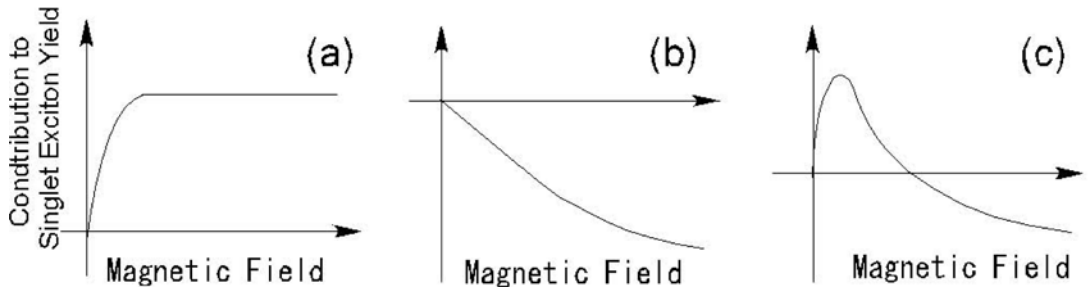
Condtribution to
Singlet Exciton Yield
(a)
Magnetic Field
(b)
Magnetic Field
(c)
Magnetic Field

FIG.1

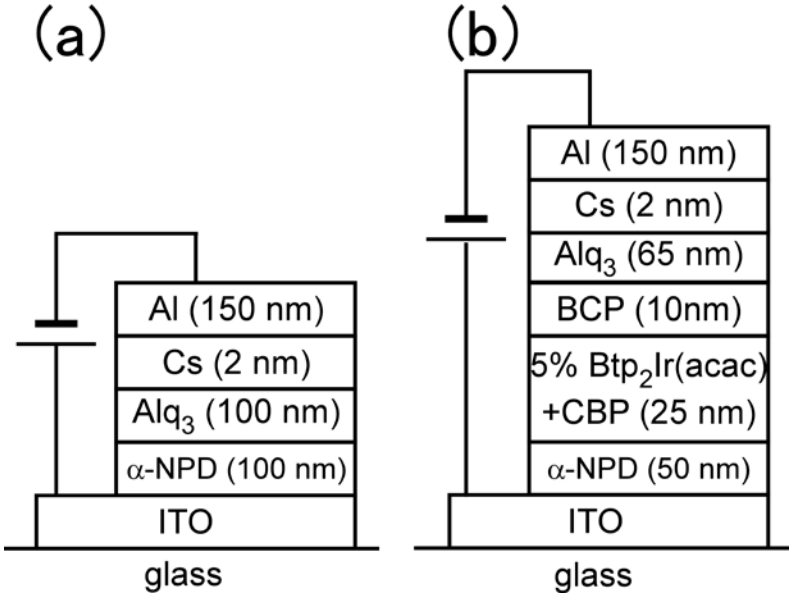
(a)
Al (150 nm)
Cs (2 nm)
Alq3 (100 nm)
α-NPD (100 nm)
ITO
glass
(b)
Al (150 nm)
Cs (2 nm)
Alq3 (65 nm)
BCP (10nm)
5% Btp2Ir(acac)
+CBP (25 nm)
α-NPD (50 nm)
ITO
glass

FIG.2

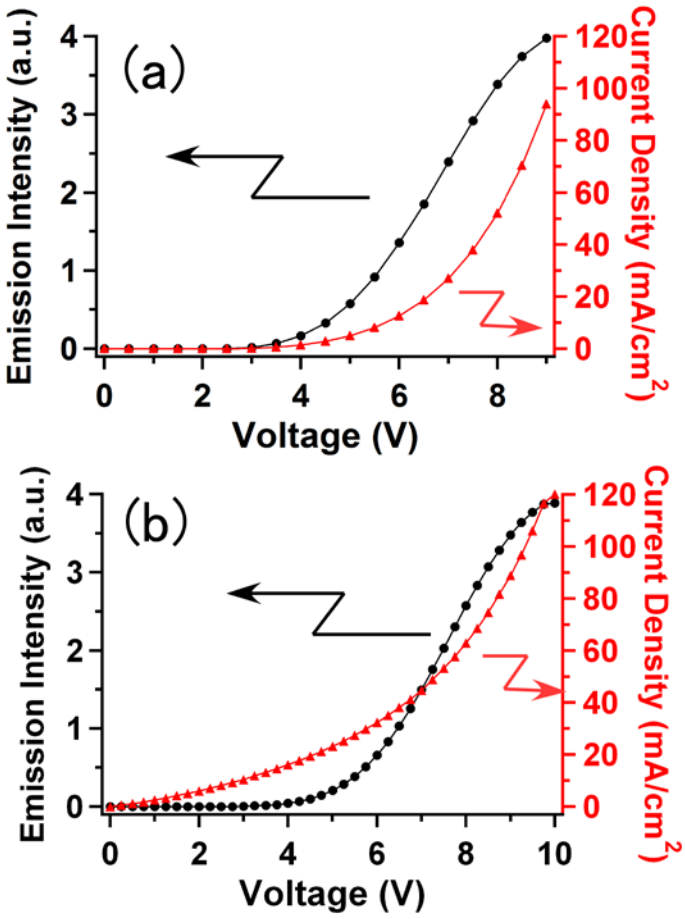
(a)
Emission Intensity (a.u.)
Current Density (mA/cm^2)
Voltage (V)
(b)
Emission Intensity (a.u.)
Current Density (mA/cm^2)
Voltage (V)

FIG.3

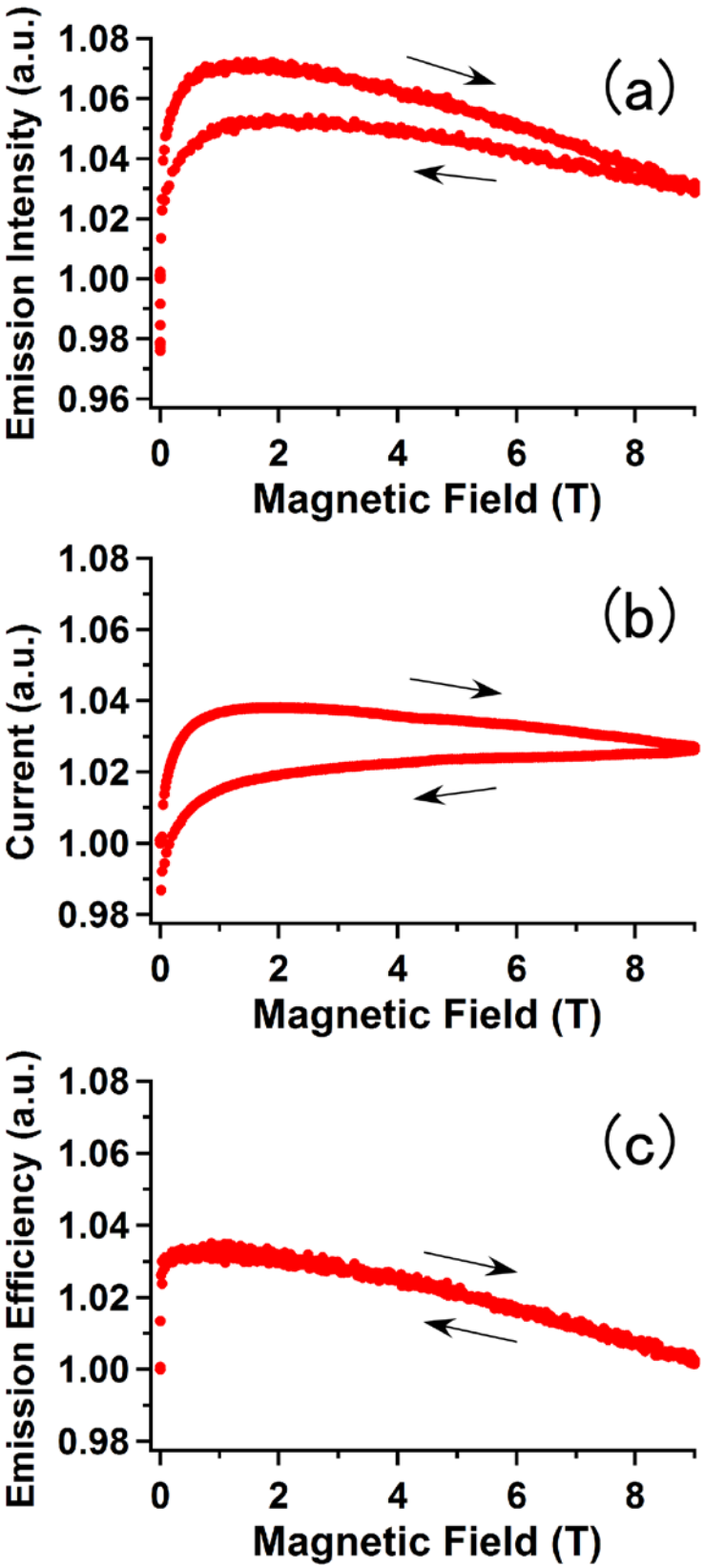
Emission Intensity (a.u.)
1.08
1.06
1.04
1.02
1.00
0.98
0.96
0
2
4
6
8
Magnetic Field (T)
(a)
Current (a.u.)
1.08
1.06
1.04
1.02
1.00
0.98
0
2
4
6
8
Magnetic Field (T)
(b)
Emission Efficiency (a.u.)
1.08
1.06
1.04
1.02
1.00
0.98
0
2
4
6
8
Magnetic Field (T)
(c)

FIG.4

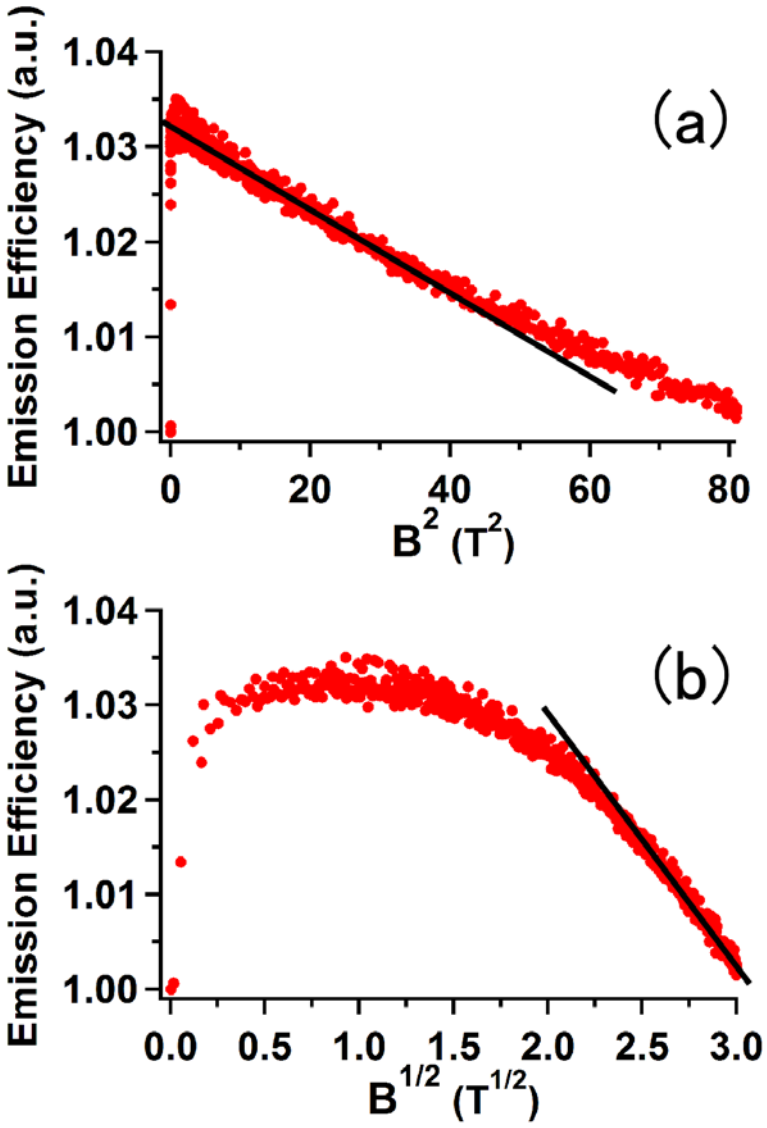
Emission Efficiency (a.u.)
1.04
1.03
1.02
1.01
1.00
(a)
0
20
40
60
80
B2 (T2)
Emission Efficiency (a.u.)
1.04
1.03
1.02
1.01
1.00
(b)
0.0
0.5
1.0
1.5
2.0
2.5
3.0
B1/2 (T1/2)

FIG.5

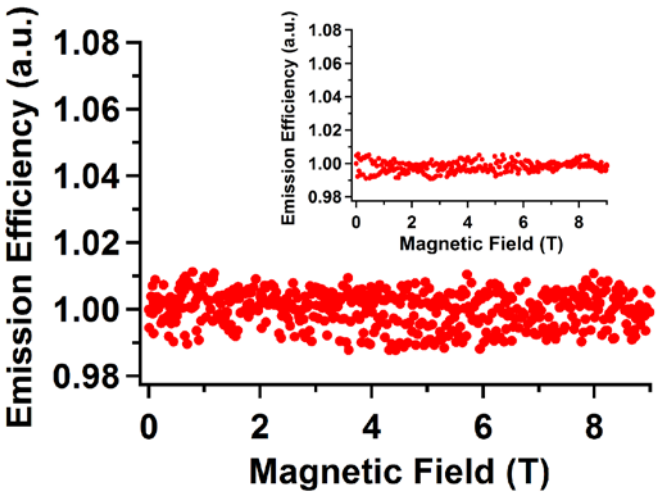
Emission Efficiency (a.u.)
1.08
1.06
1.04
1.02
1.00
0.98
0
2
4
6
8
Magnetic Field (T)
Emission Efficiency (a.u.)
1.08
1.06
1.04
1.02
1.00
0.98
0
2
4
6
8
Magnetic Field (T)

FIG.6

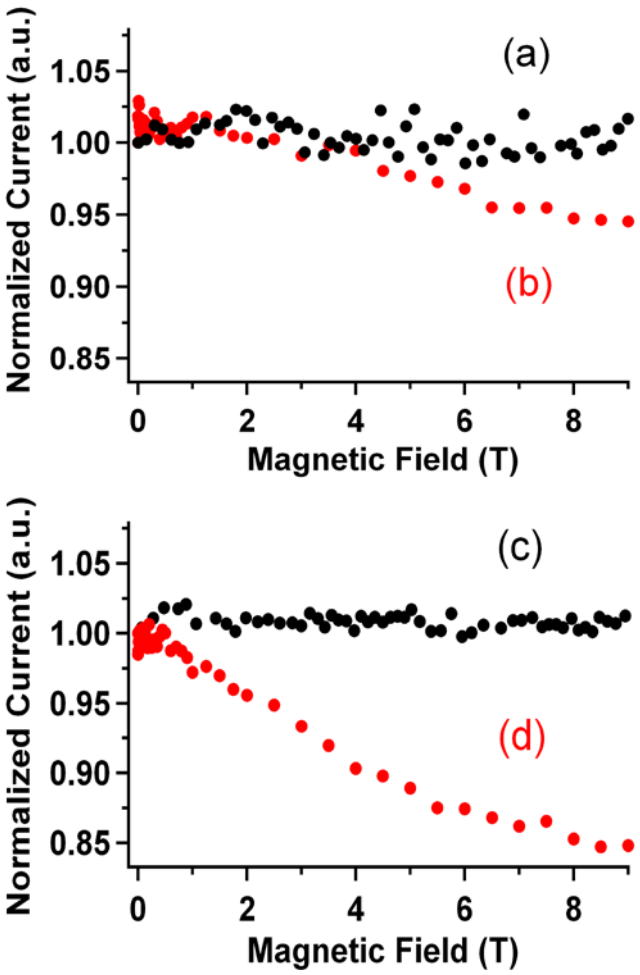
Normalized Current (a.u.)
1.05
1.00
0.95
0.90
0.85
0
2
4
6
8
Magnetic Field (T)
(a)
(b)
(c)
(d)

FIG.7